90. **Thomas, K. R., and M. R. Capecchi.** 1987. Site-directed mutagenesis by gene targeting in mouse embryo-derived stem cells. Cell **51**:503–512.
91. **Tischfield, J. A.** 1997. Loss of heterozygosity or: how I learned to stop worrying and love mitotic recombination. Am. J. Hum. Genet. **61**:995–999.
92. **Van Sloun, P. P., S. W. Wijnhoven, H. J. Kool, R. Slater, G. Weeda, A. A. van Zeeland, P. H. Lohman, and H. Vrieling.** 1998. Determination of spontaneous loss of heterozygosity mutations in Aprt heterozygous mice. Nucleic Acids Res. **26**:4888–4894.
93. **Weinstock, D. M., C. A. Richardson, B. Elliott, and M. Jasin.** 2006. Modeling oncogenic translocations: distinct roles for double-strand break repair pathways in translocation formation in mammalian cells. DNA Repair (Amsterdam) **5**:1065–1074.
94. **Wolff, S.** 1977. Sister chromatid exchange. Annu. Rev. Genet. **11**:183–201.
95. **Wu, L., and I. D. Hickson.** 2003. The Bloom's syndrome helicase suppresses crossing over during homologous recombination. Nature **426**:870–874.

Available online at www.sciencedirect.com
ScienceDirect
Advances in Space Research 40 (2007) 470–473
ADVANCES IN SPACE RESEARCH (a COSPAR publication)
www.elsevier.com/locate/asr

Influence of low-dose and low-dose-rate ionizing radiation on mutation induction in human cells

F. Yatagai [a,d,*], Y. Umebayashi [a], M. Suzuki [b], T. Abe [a], H. Suzuki [c,f], T. Shimazu [c], N. Ishioka [d,f], M. Iwaki [a], M. Honma [e]

[a] *RIKEN Institute, Wako-shi, Saitama 351-0198, Japan*
[b] *National Institute of Radiological Sciences, Chiba-shi, Chiba 263-8555, Japan*
[c] *Japan Space Forum, Chiyoda-ku, Tokyo104-0004, Japan*
[d] *Japan Aerospace Exploration Agency, Institute of Space Astronautical Science, Tsukuba-shi, Ibaraki 305-8505, Japan*
[e] *National Institute of Health Sciences, Setagaya-ku, Tokyo 158-8051, Japan*
[f] *Department of Space Environmental Medicine, Kagoshima University Graduate School of Medical and Dental Sciences, Kagoshima-shi, Kagoshima 890-8544, Japan*

Received 13 October 2006; received in revised form 8 December 2006; accepted 3 April 2007

Abstract

This is a review paper to introduce our recent studies on the genetic effects of low-dose and low-dose-rate ionizing radiation (IR). Human lymphoblastoid TK6 cells were exposed to γ-rays at a dose-rate of 1.2 mGy/h (total 30 mGy). The frequency of early mutations (EMs) in the *thymidine kinase* (*TK*) gene locus was determined to be 1.7×10^{-6}, or 1.9-fold higher than the level seen in unirradated controls [Umebayashi, Y., Honma, M., Suzuki, M., Suzuki, H., Shimazu, T., Ishioka, N., Iwaki, M., Yatagai, F., Mutation induction in cultured human cells after low-dose and low-dose-rate γ-ray irradiation: detection by LOH analysis. J. Radiat. Res., 48, 7–11, 2007]. These mutants were then analyzed for loss of heterozygosity (LOH) events. Small interstitial-deletion events were restricted to the *TK* gene locus and were not observed in EMs in unirradated controls, but they comprised about half of the EMs (8/15) after IR exposure. Because of the low level of exposure to IR, this specific type of event cannot be considered to be the direct result of an IR-induced DNA double strand break (DSB).

To better understand the effects of low-level IR exposure, the repair efficiency of site-specific chromosomal DSBs was also examined. The pre γ-irradiation under the same condition did not largely influence the efficiency of DSB repair via end-joining, but enhanced such efficiency via homologous recombination to an about 40% higher level (unpublished data). All these results suggest that DNA repair and mutagenesis can be indirectly influenced by low-dose/dose-rate IR.

Keywords: TK6 cell; Low-dose/low-dose rate γ-rays; LOH analysis

1. Introduction

It is important to study the genetic effects of low-dose/low-dose-rate ionizing radiation (IR) from the perspective of human health, because human beings are constantly exposed to low levels of IR. A higher IR background is present in a space environment where heavy charged particles are present. To reach general conclusions concerning the genetic effects of low-dose/low-dose-rate IR, large numbers of carefully designed experiments must be performed covering a wide range of doses and dose-rates. These experiments should also utilize methods which can detect both point mutations in genes and alterations in chromosomes.

* Corresponding author.
E-mail addresses: yatagai@riken.jp (F. Yatagai), m_suzuki@nirs.jp (M. Suzuki), shimazu@jsforum.jp (T. Shimazu), ishioka.noriaki@jaxa.jp (N. Ishioka), honma@nihs.go.jp (M. Honma).

0273-1177/$30 © 2007 COSPAR. Published by Elsevier Ltd. All rights reserved.
doi:10.1016/j.asr.2007.04.094

For this purpose, a new sensitive detection system has been developed using the human lymphoblastoid TK6 cell line (Honma et al., 1997).

The TK6 cell is heterozygous at the *thymidine kinase* (*TK*) locus and has been frequently used for mutation assays. The system developed here is designed for the molecular analysis of mutations located in the *TK* gene, as well as alterations at the chromosome level. This system was successfully used to detect the effects of radiation at doses as low as 100 mGy (Morimoto et al., 2002a,b). Irradiation with 100 mGy of X-rays or accelerated carbon-ions clearly demonstrated radiation-specific patterns of loss of heterozygosity (LOH), or interstitial deletions in chromosome 17. These LOH events were also detected after low-dose carbon-ion irradiation of frozen TK6 cells (Umebayashi et al., 2005). Furthermore, the ability of this detection system to measure the genetic effects of low-doses of γ-rays delivered at low-dose-rates was investigated, and the recently published results (Umebayashi et al., 2007) are introduced here.

Since LOH events can be caused by chromosomal DSBs, the influences of low-dose/low-dose-rate IR exposure on the repair of site-specific chromosomal DSBs are currently examined using the same γ-rays exposure conditions as the above mutation detection studies. Preliminary results from these studies are briefly introduced here.

2. LOH analysis for TK⁻ mutants

The outline of the experimental procedure for the detection and analysis of TK-deficient mutants is illustrated schematically in Fig. 1. The methodologies have already been reported in detail (Morimoto et al., 2002a,b). In the present experiments, TK6 cells growing in a 5% CO_2 incubator were exposed to γ-rays at a dose rate of 1.2 mGy/h

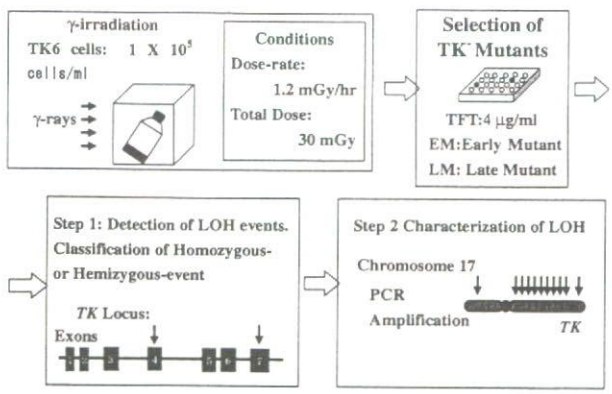

Fig. 1. Outline of the experimental procedure used for the selection and characterization of TK⁻ mutants. The γ-irradiation of TK6 cells and the selection of thymidine kinase deficient (TK⁻) mutant (EM: early selected and LM: lately selected) are schematically illustrated in the upper panel. This selection is made by the resistance to 4 μg/ml trifluorothymidine (TFT). Then, the selected mutants can be analyzed by the two steps; step 1 (judgment of LOH or non-LOH and the type of LOH) and step 2 (further characterization of LOH, so-called chromosome mapping).

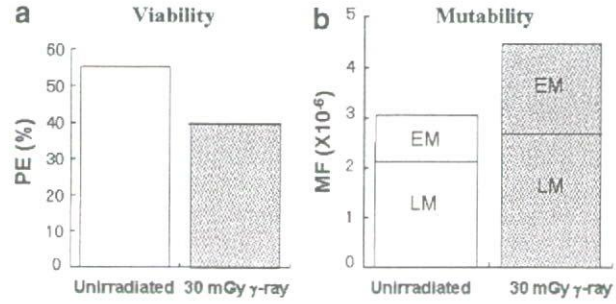

Fig. 2. Cell viability and mutability after low-dose/low-dose-rate γ-irradiation. The results have been published in the journal (Umebayashi et al., 2007).

for 25 h (for a total exposure of 30 mGy). This low-dose γ-irradiation was performed at the National Institute of Radiological Studies (NIRS). For survival assays, plating efficiency was measured with the limiting dilution method. The average value of plating efficiency (PE) decreased from 55% to 40% after γ-irradiation, but this difference is not statistically significant ($P = 0.058$: Fig. 2). The TK⁻ mutant clones were isolated by seeding cells into 96-well microwell plates at 4×10^4 cells per well, with RPMI medium containing 4 μg/ml trifluorothymidine (TFT). Early TK⁻ mutant clones (EMs) and late TK⁻ mutant clones (LMs) were selected separately after two and four weeks of incubation in this selection medium, respectively. The mutation assays showed an increase in the frequency of EMs after γ-irradiation, from 0.90×10^{-6} to 1.7×10^{-6} (Fig. 2). This is an approximately 1.9-fold increase in TK mutations, and is statistically significant ($P = 0.040$). The frequencies of LMs did not show a significant increase after γ-irradiation: 2.1×10^{-6} in unirradiated controls to 2.7×10^{-6} in irradiated cells ($P = 0.55$). The mutagenic effect of γ-irradiation was observed only in the increase of EMs.

As shown in Fig. 1, the selected TK⁻ mutants were analyzed to determine the loss of *TK* heterozygosity (LOH)

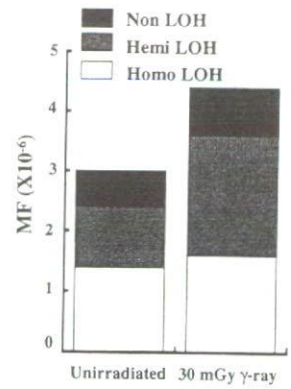

Fig. 3. Classification of TK⁻ mutants. All mutants including EM and LM are classified by PCR amplification test (see text). The results have been published in the journal (Umebayashi et al., 2007).

using PCR amplification of the exon 4 and 7 regions of the *TK* locus (Honma et al., 1997). If both regions can be amplified by PCR in a manner similar to that seen in the parental TK heterozygous cells, this type of mutant is classified as a "non LOH" mutant. This type of PCR amplification can also distinguish two types of LOH, homozygous and hemizygous, in which the functional *TK* allele is either replaced by the mutated TK^- allele or lost, respectively. The homozygous and hemizygous types of LOH mutations can be considered to be the result of homologous recombination (HR) repair or end-joining (EJ) repair of DNA double-strand breaks (DSBs), respectively. The frequency of hemizygous LOH mutations (1.0×10^{-6} to 2.1×10^{-6}) (Fig. 3) was changed by γ-irradiation. This increase is clearly due to the difference in the efficiency in the recovery of EMs [EM/(EM + LM); 0/13 and 8/19 for unirradiated controls and the γ-irradiated cells, respectively]. For additional information on the extent of the deleted or substituted portions of the chromosome in the LOH mutants, 11 microsatellite regions (D17S588, D17S1784, D17S785, D17S789, D17S802, D17S807, D17S928, D17S932, D17S1299, D17S1566 and THRA) were analyzed on chromosome 17 using multiple PCR reactions as described previously (Yatagai et al., 2004). The deleted or replaced regions of chromosome 17 in each LOH mutant are shown by a shaded region in each column in Fig. 4. Type 2 hemizygous events (interstitial deletions), exhibiting a small size deletion restricted to the *TK* locus, were frequently observed in the EM group after γ-irradiation (8/15). In contrast, there was no detection of this type of event among the EMs in the unirradiated controls (and only a single event detected in the LM group). This result also

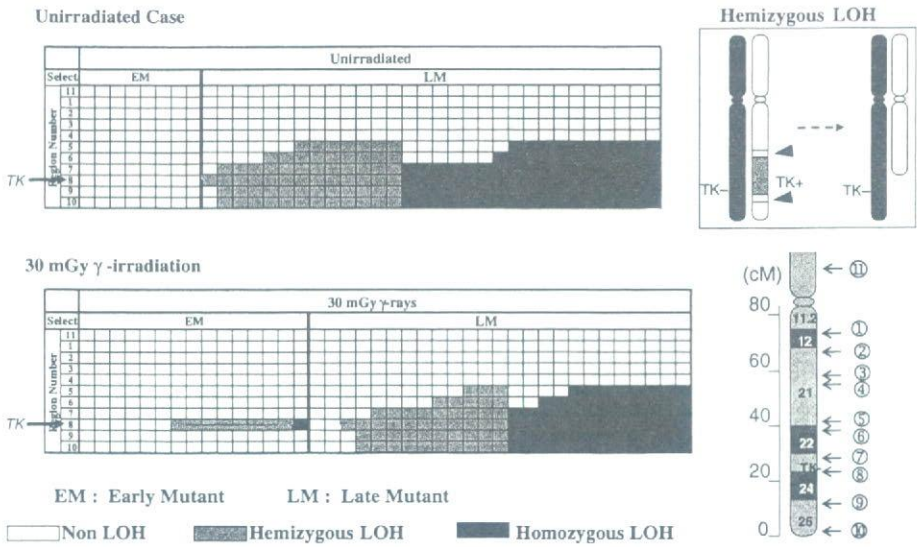

Fig. 4. Characterization of TK^- mutants. (Chromosome mapping of LOH mutants.) The results have been published in the journal (Umebayashi et al., 2007).

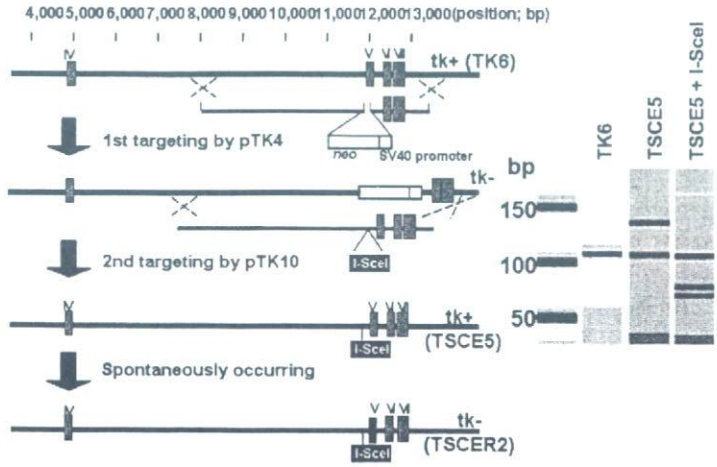

Fig. 5. Establishing the TSCE5 and TSCER2 cell lines using two step gene targeting. The details of gene-targeting procedures have been described in the journal (Honma et al., 2003).

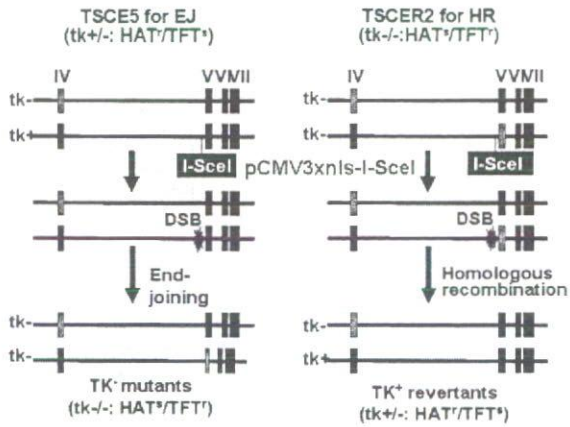

Fig. 6. Strategy for detecting DSB repair through homologous recombination (HR) and non-homologous end-joining (EJ). The details of strategy have been described in the journal (Honma et al., 2003).

provides support for the idea that the mutagenic effects of low dose and low dose rate γ-irradiation in this system are measured by the resulting EMs.

3. Analysis for repair of site-specific DSB

Considering the above results from genetic analysis together with the estimated low probability for the formation of a DSB in the *TK* locus region, 2.25×10^{-10} (Umebayashi et al., 2007), radiation-induced DSBs seem unlikely to be directly involved in the observed enhancement of specific interstitial-deletion events. Instead, it seems probable that such low-level IR exposure might affect the repair of spontaneously occurring DSBs. In order to explore this possibility, an attempt was made to use a recently constructed model system to investigate the fate of DSBs (Honma et al., 2003). An 18 bp sequence containing the recognition site for the restriction enzyme I-SceI was introduced into the region upstream of exon 5 in the TK^+ allele of TK6 cells. The cells containing this insert were designated TSCE5 (Fig. 5). In addition, a compound heterozygote ($TK^{-/-}$) cell line, TSCER2 was obtained by a spontaneous reversion in a TSCE5 cell clone (G to A in the 23rd base position of exon 5). When a DSB at the I-SceI site is repaired by EJ in TSCE5, it causes a deletion, permitting the cell to be isolated as a TK-deficient mutant. In TSCER2, on the other hand, when the DSB is repaired by HR between *TK* alleles, a TK^+ allele is generated resulting in a revertant phenotype (Fig. 6). Preliminary results are described briefly here concerning the influence of low-level IR exposure on DSB repair using this system. After the transfection of a I-SceI expression vector, pCMV3xnls-I-SceI, the occurrence of mutants in TSCE5 cells and revertants in TSCER2 cells were measured, and these were found at a frequency of 10^{-3}–10^{-2} and 10^{-5}–10^{-4}, respectively. From the comparison of both of these frequencies in unirradiated controls, it appears that EJ contributes to the repair of DSBs about 70-fold more efficiently than HR. This fact is consistent with the approximately 100-fold higher efficiency for EJ observed in our previous experiment (Honma et al., 2003). The low-dose/low-dose-rate γ-irradiation (a total of 30 mGy at 1.2 mGy/h) appeared to have almost no influence on EJ, but the efficiency of HR was enhanced about 40% by the γ-irradiation. However, this preliminary result is not consistent with the enhancement of EJ-mediated events observed with the above LOH analysis. Although there is a discrepancy between the LOH analysis and the DSB repair assay, this I-SceI system, which is still being refined, should be useful as a model system for studies of repair of single DSBs which occur spontaneously or are induced by low-dose IR exposure.

Acknowledgments

This study was partially supported by the Budget for Nuclear Research of the Ministry of Education, Culture, Sports, Science and Technology, and was reviewed by the Atomic Energy Commission.

References

Honma, M., Zhang, L.S., Hayashi, M., Takeshita, K., Nakagawa, Y., Tanaka, N., Sofuni, T. Illegitimate recombination leading to allelic loss and unbalanced translocation in p53-mutated human lymphoblastoid cells. Mol. Cell. Biol. 17, 4774–4781, 1997.

Honma, M., Izumi, M., Sakuraba, M., Tadokoro, S., Sakamoto, H., Wang, W., Yatagai, F., Hayashi, M. Deletion, rearrangement, and gene conversion; genetic consequences of chromosomal double-strand breaks in human cells. Environ. Mol. Mutagen 42, 288–298, 2003.

Morimoto, S., Kato, T., Honma, M., Hayashi, M., Hanaoka, F., Yatagai, F. Detection of genetic alterations induced by low-dose X rays: analysis of loss of heterozygosity for TK mutation in human lymphoblastoid cells. Radiat. Res. 157, 533–538, 2002a.

Morimoto, S., Honma, M., Yatagai, F. Sensitive detection of LOH events in a human cell line after C-ion beam exposure. J. Radiat. Res. 43 (Suppl.), S163–S167, 2002b.

Umebayashi, Y., Honma, M., Abe, T., Ryuto, H., Suzuki, H., Shimazu, T., Ishioka, N., Iwaki, M., Yatagai, F. Mutation induction after low-dose carbon-ion beam irradiation of frozen human cultured cells. Biol. Sci. Space 19, 237–241, 2005.

Umebayashi, Y., Honma, M., Suzuki, M., Suzuki, H., Shimazu, T., Ishioka, N., Iwaki, M., Yatagai, F. Mutation induction in cultured human cells after low-dose and low-dose-rate γ-ray irradiation: detection by LOH analysis. J. Radiat. Res. 48, 7–11, 2007.

Yatagai, F., Morimoto, S., Kato, T., Honma, M. Further characterization of loss of heterozygosity enhanced by p53 abrogation in human lymphoblastoid TK6 cells: disappearance of endpoint hotspots. Mutat. Res. 560, 133–145, 2004.

Available online at www.sciencedirect.com
ScienceDirect
Mutation Research 638 (2008) 48–55
Fundamental and Molecular Mechanisms of Mutagenesis
www.elsevier.com/locate/molmut
Community address: www.elsevier.com/locate/mutres

Mutagenic radioadaptation in a human lymphoblastoid cell line

Fumio Yatagai [a,*], Yukihiro Umebayashi [a], Masamitsu Honma [b], Kaoru Sugasawa [c], Yuko Takayama [a], Fumio Hanaoka [d]

[a] *Advanced Development and Support Center, The Institute of Physical and Chemical Research (RIKEN), Saitama 351-0198, Japan*
[b] *Division of Genetics and Mutagenesis, National Institute of Health Sciences, Tokyo 158-8501, Japan*
[c] *Genome Damage Response Research Unit, The Institute of Physical and Chemical Research (RIKEN), Saitama 351-0198, Japan*
[d] *Graduate Program, Frontiers in Biosciences, Osaka University, Osaka 565-0871, Japan*

Received 6 April 2007; received in revised form 15 August 2007; accepted 22 August 2007
Available online 1 September 2007

Abstract

We investigated the mutagenic radioadaptive response of human lymphoblastoid TK6 cells by pretreating them with a low dose (5 cGy) of X-rays followed by a high (2 Gy) dose 6 h later. Pretreatment reduced the 2-Gy-induced mutation frequency (MF) of the *thymidine kinase* (*TK*) gene (18.3×10^{-6}) to 62% of the original level (11.4×10^{-6}). A loss of heterozygosity (LOH) detection analysis applied to the isolated TK^- mutants revealed the mutational events as non-LOH (resulting mostly from a point mutation in the *TK* gene), hemizygous LOH (resulting from a chromosomal deletion), or homozygous LOH (resulting from homologous recombination (HR) between chromosomes). For non-LOH events, pretreatment decreased the frequency to 27% of the original level (from 7.1×10^{-6} to 1.9×10^{-6}). cDNAs prepared from the non-LOH mutants revealed that the decrease was due mainly to the repression of base substitutions. The frequency of hemizygous LOH events, however, was not significantly altered by pretreatment. Mapping analysis of chromosome 17 demonstrated that the distribution and the extent of hemizygous LOH events were also not significantly influenced by pretreatment. For homozygous LOH events, pretreatment reduced the frequency to 61% of the original level (from 5.1×10^{-6} to 3.1×10^{-6}), reflecting an enhancement in HR repair of DNA double-strand breaks. Our findings suggest that the radioadaptive response in TK6 cells follows mainly from mutations at the base-sequence level, not the chromosome level.

Keywords: Adaptive response; TK6 cells; LOH detection system

1. Introduction

An adaptive cellular response occurs when a mild stress applied before a challenging treatment with a DNA-damaging agent decreases the detrimental effects of the challenge. In radioadaptation, as it is usually defined, exposure to a low dose of ionizing radiation (IR) provides some protection against a high dose. Radioadaptation was first reported by Olivieri et al. [1], who showed that radiation delivered by labeling human lymphocytes with tritiated thymidine causes a decrease in the frequency of chromosomal aberrations induced by subsequent exposure to 15 Gy of IR. That discovery stimulated a series of studies in human lymphocytes and various mammalian cell lines (for review, see refs. [2,3]) and suggested that the adaptive response is an important defense mechanism, especially against low doses of IR. The molecular mechanisms involved, however, remain largely unknown [4–8], and cellular

* Corresponding author. Tel.: +81 48 467 9710; fax: +81 48 462 1426.
E-mail address: yatagai@postman.riken.go.jp (F. Yatagai).

0027-5107/$ – see front matter © 2007 Elsevier B.V. All rights reserved.
doi:10.1016/j.mrfmmm.2007.08.014

responses such as the bystander effect, genetic instability and hyper-radiosensitivity seem tightly related to the adaptive response in a specific low-dose region. One of the hot subjects in recent adaptive response studies is the expression of the genes involved in the mechanism [8–10]. Another is the relationship between the adaptive response and the bystander effect [11–15]. In mammalian cells, for example, bystander mutagenesis may be suppressed by an adaptive response [11].

Following the report by Olivieri et al., reduced induction of both micronuclei and sister chromatid exchanges was shown in Chinese hamster V79 cells pre-exposed to low doses of γ-rays or ^{3}H β-rays [16]. Subsequent studies reported similar radioadaptive responses, such as reduced mutation frequencies in human lymphocytes [17], mouse SR-1 cells [18] and human–hamster hybrid A_L cells [19], an altered mutation spectrum in human–hamster hybrid A_L cells [19], reduced micronucleus frequencies in human lymphocytes [5] and mouse embryo cells [20], and reduced deletions and rearrangements in human lymphoblast cells [21]. The mechanism underlying those radioadaptations may have been the induction of an efficient chromosome repair system by the priming radiation dose, and in fact, the efficiency of DNA double-strand break (DSB) repair in Chinese hamster V79 cells exposed to γ-rays is enhanced by a priming exposure of 5 cGy of γ-rays [22]. Furthermore, DSBs with either blunt or staggered ends, created by restriction enzymes, induce the adaptive response [3].

The human lymphoblastoid TK6 cell line, isolated by Skopek et al. [23], is heterozygous at the *thymidine kinase* (*TK*) locus. Honma's laboratory developed a loss of heterozygosity (LOH) detection system that can be used for molecular analysis of *TK* mutations as well as for detecting alterations at the chromosome level [24,25]. Using that methodology, we were able to detect IR effects at doses as low as 10 cGy [26–28]. Irradiation of TK6 cells with 10 cGy of X-rays clearly demonstrated radiation-specific types of LOH events or interstitial deletions in chromosome 17 [26]. We also observed more efficient induction of such events after 10 cGy irradiation with an accelerated carbon-ion (135 MeV/u) beam [27], and this was apparent in frozen cells exposed to the same carbon-ion beam [28]. These results strongly suggest that the interstitial deletions were the result of end-joining repair of IR-induced DSBs.

Because the radiation-sensitive LOH analysis system in TK6 cells is effective for detecting the fate of radiation-induced DNA double-strand breaks (DSBs), we use it here to see if the adaptive response could produce measurable changes in IR-induced genetic alterations. The results we obtained were not completely expected, but are interesting.

2. Materials and methods

2.1. Cell culture and adaptive treatment

The methodologies for the detection of *TK*-deficient mutants and the materials and methods used for cell culture and growth have been previously reported [26]. Briefly, TK6 cells were incubated in RPMI1640 medium supplemented with HAT to eliminate pre-existing TK^- deficient mutants. The cells were then resuspended in fresh normal medium, and 6 ml cell suspension was dispensed into 6-cm diameter Petri dishes. The cells were pretreated ("primed") with 2.5, 5 or 10 cGy of X-rays (250 kVp) at a rate of 10 cGy/min, and placed in a 5% CO_2 humidified incubator. The cell concentration was adjusted to 8×10^5 cells/ml at the end of the post-irradiation incubation period of 1.5, 3, 6, 9 or 12 h. The cells were then challenged with 2 Gy X-rays (250 kVp) at 1 Gy/min. Non-primed irradiated cells treated in the same manner as the primed cells served as controls.

2.2. Survival assay and TK mutation assay

To determine the surviving fraction of the challenged cells, we measured the plating efficiency (PE) immediately after irradiation using the limiting dilution method. For mutation expression, we incubated the cells with non-selecting RPMI1640 medium for about 60 h following the X-ray challenge. We measured the PE of incubated cells similarly, determining the *TK* mutation frequency. To select TK^- mutant clones, we seeded incubated cells into 96-well plates at 4×10^4 cells per well in RPMI1640 medium containing 4 μg/ml trifluorothymidine (TFT); we harvested the normally growing clones after 2 weeks and the slow growing clones after 4 weeks.

2.3. Determination of optimum irradiation conditions for mutagenic adaptation

To determine the optimum conditions for evoking the mutagenic radioadaptive-response, we tested the MF induced by 2 Gy at 0, 1.5, 3, 6, 9 and 12 h after a priming dose of 10 cGy, selected the optimum interval time, and then tested the MF induced by 2 Gy at that interval time after priming doses of 0, 2.5, 5 and 10 cGy.

2.4. LOH analysis of TK^- mutants

Fig. 1 illustrates how we classified TK^- mutants. We first determined *TK* LOH by PCR analysis of exons 4 and 7 [29]. If the PCR products of both were similar to those of the parental *TK* heterozygous cells, we classified the mutant

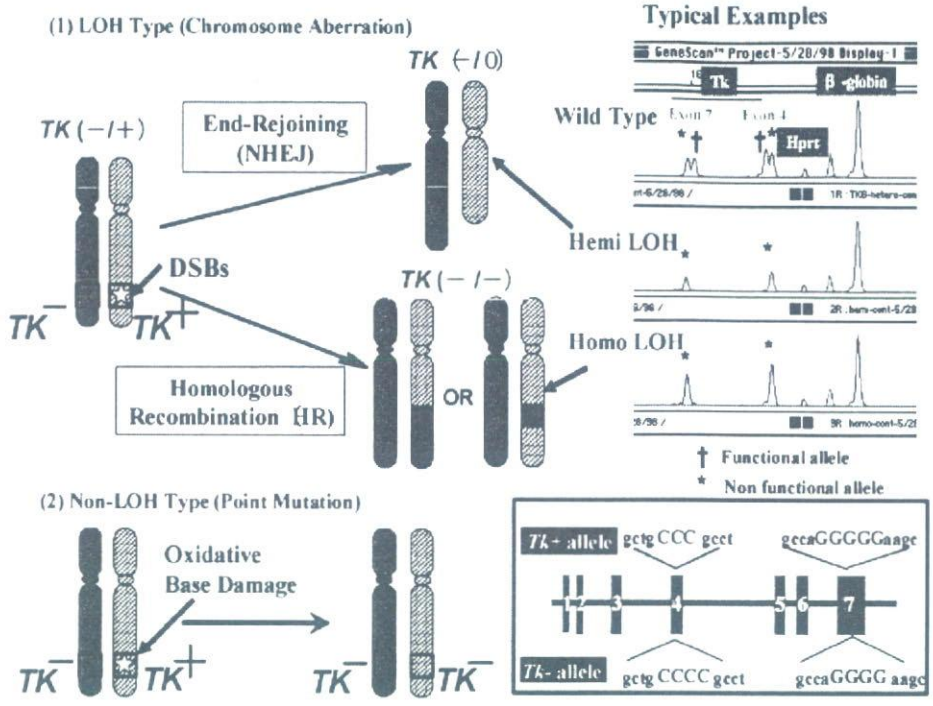

Fig. 1. LOH classifications of *TK*$^{-}$ mutants. The first step in the genetic analysis of selected *TK*$^{-}$ mutants was to judge whether there was a loss of *TK* heterozygosity (LOH). This was accomplished by PCR amplification of exons 4 and 7 regions of the *TK* locus. This step also distinguished between hemizygous LOH (loss of the functional *TK* allele) and homozygous LOH (replacement of the functional *TK* allele by a mutated *TK*$^{-}$ allele (see ref. [29]).

as a "non-LOH" mutant. We used the same technique to distinguish between hemizygous LOH (in which the functional *TK* allele is lost) and homozygous LOH (in which the functional *TK* allele is replaced by *TK*$^{-}$). To determine the extent and size of the deleted or substituted portions of the chromosome involved, we analyzed 11 microsatellite regions (D17S588, D17S1784, D17S785, D17S789, D17S802, D17S807, D17S928, D17S932, D17S1299, D17S1566 and THRA) on chromosome 17 using multiple PCR reactions as described previously [29]. The fine structure of the recovered *TK*$^{-}$ LOH mutations was determined by chromosome mapping analysis.

2.5. Base sequencing of non-LOH mutants

For a precise analysis of non-LOH mutants, we extracted RNA using Isogen (Nippon Gene, Japan), and obtained cDNA using a First-Strand cDNA Synthesis Kit, Amersham, USA). Following PCR amplification, the purified 807-bp fragments were sequenced by Takara Bio (Japan). The primers 5′-AGAGTACTCGGGTTCGTGAA-3′ and 5′-GCAGCATGCAGGGCAGCGTG-3′ (forward and reverse, respectively) were used for cDNA synthesis, PCR amplification and base sequencing [30]. To prevent the overestimation of mutational events, we counted identical mutations originating from a single irradiated dish as a single event.

Table 1a
TK mutation frequency (MF) at various time intervals between priming and challenging X-ray exposures (priming dose, 10 cGy; challenging dose, 2 Gy)

Time interval (h)	0	1.5	3	6	9	12
TK MF ($\times 10^{-6}$)	19.8	18.1	14.4	13.5	17.8	19.7

3. Results

3.1. Optimum conditions for mutagenic adaptation

For inducing an adaptive response to X-ray irradiation, the optimum interval between a 10-cGy priming dose and a 2-Gy challenging dose was 6 h (Table 1a), and the optimum priming dose 6 h prior to a 2-Gy challenging dose was 5 cGy (Table 1b). We therefore decided to characterize the induced *TK* mutants by repeating

Table 1b
TK mutation frequency at various priming X-ray doses (challenging dose, 2 Gy; interval between 2 exposures, 6 h)

Priming X-ray dose (cGy)	0	2.5	5	10
TK MF ($\times 10^{-6}$)	13.3	15.8	4.5	6.3

Table 2
Surviving fractions of primed and non-primed TK6 cells following challenge exposure to 2 Gy X-rays

Experiment	Surviving fraction	
	Non-primed cells	Primed cells (5 cGy)
I	0.043	0.047
II	0.047	0.070
III	0.049	0.040
Mean ± S.D.	0.046 ± 0.0031*	0.052 ± 0.016*

* $P = 0.58$; t-test.

Table 3
TK mutation frequency in primed and non-primed TK6 cells following challenge exposure to 2 Gy X-rays

Experiment	*TK* mutation frequencies ($\times 10^{-6}$)	
	Non-primed cells	Primed cells (5 cGy)
I	13.3	4.5
II	13.3	10.5
III-a	20.4	15.1
III-b	21.0	15.6
Mean ± S.D.	18.3 ± 4.3*	11.4 ± 5.1*

Experiments III-a and III-b were carried out concurrently with survival assay III, but they were independent mutation assays.
* $P = 0.020$; t-test.

our mutation experiments under those conditions (5 cGy followed 6 h later with 2 Gy).

3.2. Survival assay and TK mutation assay

Table 2 shows the surviving fraction, expressed as PE (2 Gy X-ray irradiated cells)/PE (unirradiated cells) of primed and unprimed cells immediately after the 2-Gy challenge exposure. Irradiation with the priming dose of 5 cGy did not influence the PE of unchallenged cells (data not shown). The effect of priming on survival after 2 Gy X-ray irradiation was 1.1 (0.052/0.046; $P = 0.58$, t-test). Thus, priming did not significantly affect survival after the challenge exposure.

On the other hand, priming did affect the *TK* MF induced by the challenge. Data from 4 independent experiments showed that priming reduced the MF to 62% of the unprimed MF ($P = 0.020$, t-test) (Table 3).

3.3. LOH analysis of TK^- mutants

Table 4 shows the distributions of LOH classes among the isolated TK^- mutants as determined by PCR analysis. We isolated non- and "small" LOH mutants (see Sections 3.4 & 3.5) as normal growth mutants in the first selection, except for a few cases. We isolated the remaining LOH mutants as slow growth mutants in the second selection. We estimated the pre-exposure effect from the proportion of each mutational event as follows: (i) 7.1×10^{-6} to 1.9×10^{-6} reduction in corresponding MF of non-LOH events, (ii) 6.4×10^{-6} to 6.1×10^{-6} change in corresponding MF of hemizygous LOH events and (iii) 5.1×10^{-6} to 3.1×10^{-6} reduction in corresponding MF of homozygous LOH events. Thus, the MF of a non-LOH event in primed cells was reduced to 27% of the non-primed MF. The induction of hemizygous events, on the other hand, was barely influenced by priming. As far as homozygous events go, their corresponding MF was reduced to 61% of the original level, which was similar to level of reduction in total MF (62%).

3.4. Analysis of LOH tracts on chromosome 17

Fig. 2 shows the deleted or replaced regions of chromosome 17 in each LOH mutant. Mutants reflected both type 1 and type 2 LOH events. Type 1 defines a terminal event; that is, the deleted or exchanged chromosome segment extends to the telomere marker (D17S928). Type 2 defines an interstitial deletion; the altered segment does not reach the telomere marker.

In the present study, most hemizygous LOH mutations, which are considered to be the result of DSB non-homologous end-joining (NHEJ) repair, reflected

Table 4
Distribution of mutational classes among the isolated *TK* mutants

Mutational class	Number of identified mutants (Exp. I, II, III-a, III-b) [MF $\times 10^{-6}$]	
	Non-primed cells	Primed cells (5 cGy)
Non-LOH	18 (5, 4, 6, 3) [7.1]	8 (1, 3, 2, 2) [1.9]
LOH		
Hemizygous	15 (3, 3, 7, 2) [6.0]	27 (8, 7[a], 5, 7) [6.4]
Homozygous	13 (3, 4, 3, 3) [5.1]	13 (2, 3, 5, 3) [3.1]
Total	46 (11, 11, 16, 8) [18.3]	48 (11, 13, 12, 12) [11.4]

[a] One of the seven mutants was a mixed hemizygous/homozygous type.

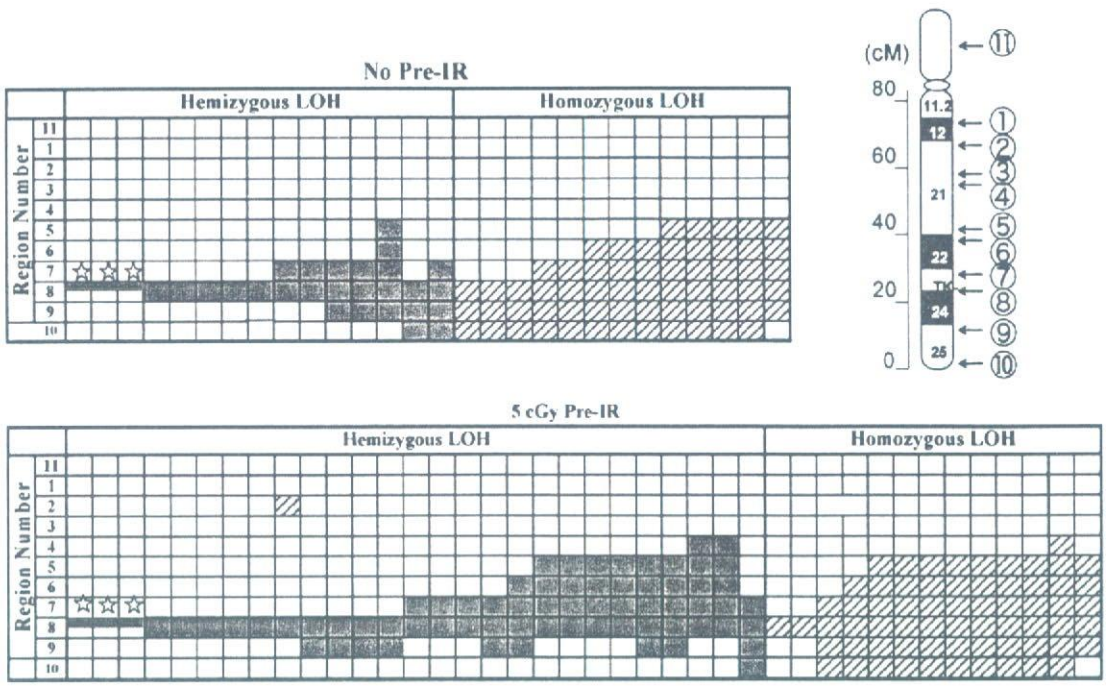

Fig. 2. Chromosome mapping of the LOH mutants. We analyzed the LOH mutants selected after a 2 Gy of challenging X-ray irradiation to determine the extent of the deleted or exchanged portions of the chromosome. The upper panel shows the profiles of 28 LOH mutants selected from non-primed cells, and the lower panel shows the profiles of 40 LOH mutants selected from cells primed with 5 cGy of X-rays. Each column represents a single LOH mutant. The rows represent regions of chromosome 17 diagrammed in the upper right insert. Shaded squares represent deleted regions and hatched squares represent exchanged regions (see text). The region numbers refer to the 11 microsatellite regions: (1) D17S588; (2) D17S1784; (3) D17S785; (4) D17S789; (5) D17S802; (6) D17S807; (7) D17S928; (8) D17S932; (9) D17S1299; (10) D17S1566; (11) THRA (see ref. [29]). The star symbol represents a "small" type 2 hemizygous event in which the deletion is restricted to *TK* locus.

type 2 events in both the non-primed (13 of 15 mutants) and primed (26 of 27 mutants) groups. Small type 2 deletions – those restricted to the *TK* locus (Fig. 2) – were infrequent in both groups (3 of 15 mutants in non-primed cells and 3 of 27 in primed cells). Similarly, the proportion of large deletion mutants (expanding to the region beyond region 8, Fig. 2) was also similar in the primed (18 of 27 mutants) and non-primed (7 of 15 mutants) groups. Homozygous LOH events, on the other hand, which are considered to be the result of homologous recombination (HR) repair of DSBs, were primarily identified as type 1 events in both primed (10 of 13) and non-primed (12 of 13) groups. Interestingly, small homozygous LOH events (where only a single region was replaced, Fig. 2) were recovered from the primed cells (2 of 13 (3 0f 14)), but not from the non-primed cells (0 of 13).

3.5. Analysis of non-LOH-mutants

We detected many types of alterations in the non-LOH mutant cDNAs (Table 5). The proportion of single base-substitutions among all the mutations identified as this class was 1/8 (13%) in the primed cells, and this value was clearly lower than 7/18 (87%) in the unprimed cells. G and C bases were targeted in base substitution mutations, except for a single case of an A to T transversion (Table 5). Most (4/5) of the double-base changes consisted of a single base deletion (causing a frameshift) and a base substitution, except for a single case of a GC to TA double transversion in a radioadapted mutant. It is difficult to estimate the effect of priming on the induction of the double-base change events from the limited number of cells involved. Similar difficulties were also found in the other mutational events in this class such as triple-base changes, multiple-base changes and exon skipping. In addition, the proportion of abnormal transcription events (both functional and non-functional *TK* alleles are equally transcribed) was also similar in the radioadapted (1/8, 13%) and the non-adapted (3/18, 17%) group, although its origin was not identified.

4. Discussion

The radioadaptation conditions used in this study (5 cGy of priming X-rays followed in 6 h by 2 Gy of challenging X-rays) were similar to those used in other studies [4,6,11,12,14,16]. The *TK* mutation frequency

Table 5
Nature of the isolated non-LOH mutants

Type of mutation		Number of identified mutants	
Specific changes	[Position: exon]	Non-primed exposure	Primed (5 cGy) pre-X-ray
Single base substitutions		7	1
G → A (Gly → Glu)	[56:1]	3	0
C → T (Gln → Stop)	[64:1]	1	0
C → A (Ser → Stop)	[89:2]	1	0
A → T (Ser → Cys)	[97:2]	1	0
G → C (Leu → Phe)	[108:2]	0	1
G → A (Glu → Lys)	[430:6]	1	0
Double base changes		3	2
G → A (Gly → Glu)/Del. C	[56:1/676:7]	1	0
G → C (Leu → Phe)/Del. A	[108:2/686:7]	0	1
Add. C/Del. G	[232:4/641:7]	1	0
GC → TA (Leu Asp → Leu Asn)	[372 and 373:5]	0	1
G → A (Glu → Lys)/Del. G	[430:6/447:6]	1	0
Triple base changes		0	1
Del. G/C → T (Ile → Ile)/C → T (Leu → Leu)	[92:1/288:4/561:7]	0	1
Multiple base changes		1	1
CC → AT (Thr Gln → Thr Stop)/G → A (Gln → Gln)/G → A (Gln → Gln)/Add. C/Del. G	[51 and 52:1/66:1/667:7/232:4/641:7]	0	1
Base changes at 20 sites		1	0
Exon skipping, abnormal splicing and deletion		3	2
Del. of a part of exon 1 (48 bases)	[161–209: 1]	1	1
Abnormal splicing of intron (between exons 1 and 2)		1	0
Skipping of exon 3 (Del. 111 bases)	[99–203: 3]	1	0
Skipping of exon 5 (Del. 90 bases)	[304–393: 5]	0	1
Abnormal transcription		3	1
Both functional and non-functional alleles are equally transcribed			
Unidentified		1	0
Total		18	8

we observed after the challenge X-rays (18.3×10^{-6}) was reduced by the 5-cGy priming exposure to about 62% of the non-primed level (11.4×10^{-6}). Taking into consideration the *TK* spontaneous mutation frequency observed in our recent study (3.0×10^{-6}) [32], the increase in MF induced by 2 Gy of X-rays was reduced from 6.1-fold to 3.8-fold.

We originally planned this study to determine whether radioadaptation would alter the characteristics of X-ray-induced LOH events. X-ray-induced interstitial deletions are likely to be the result of NHEJ repair of DSBs, and this type of mutation was the one we recovered most frequently after 2 Gy X-ray irradiation in our previous study [24]. We also found that carbon-ion beam irradiation induced interstitial deletions more efficiently than the same dose of X-rays [26,27], which we interpreted as the result of a higher occurrence of inaccurately repaired DSBs. In the present study, however, we found that the frequency of hemizygous LOH mutations, as well as their size and the distribution of deleted regions on chromosome 17, was similar for radioadapted and non-adapted cells. Those results are not consistent with reports suggesting that enhanced repair of DSBs reduces chromosomal alterations [21,22]. An entire genome assay might lead to results similar to the ones in those reports, but our observations were restricted to the *TK* locus on chromosome 17.

On the other hand, we observed a decrease in the induction of homozygous LOH events in the primed cells, which suggests that priming enhanced the HR repair of DSBs. We recently constructed a model system to follow the fate of a single DSB introduced by the restriction enzyme I-sceI at a specific site in the *TK* gene in TK6 cells [31]. In preliminary exper-

iments, low dose/low-dose rate γ-irradiation (30 mGy at 1.2 mGy/h) did not significantly affect end joining (EJ) repair of this specific DSB, but it enhanced the efficiency of HR repair by about 50% (unpublished data). The small homozygous LOH events we observed in the primed cells in the present study (3/14) might reflect this enhanced HR, but we must examine whether the adaptive response was really involved because we also recovered small homozygous LOH mutants after the low-dose/low-dose rate γ-ray exposures [32]. The decrease in the frequency of single-base substitutions that we observed in primed cells (1/48) versus non-primed cells (7/46) (Tables 4 and 5) is rarely influenced by counting base substitutions accompanied by single base deletions (which would result in 2/48 for primed cells and 9/46 for non-primed cells), so the most likely mechanism for the reduced induction of non-LOH mutants was suppression of base substitutions.

One of the possible targets for radioadaptation is oxidative base damage. In fact, down-regulation of the human *CDC16* gene that occurs after oxidative stress causes more rapid and efficient repair in adapted (2 cGy pre-irradiated) human lymphoblastoid cells challenged with 4 Gy irradiation [6]. On the other hand, oxidative base excision repair enzymes, including DNA glycosylases, hOGG1 and hNth1, are reportedly not up-regulated at the post-transcriptional level in γ-ray-primed TK6 cells [33]. Since DNA glycosylase can suppress base substitution, we need to examine whether radioadaptation enhances the enzyme's activity under the present condition. Alternatively, base substitution activity might not accurately reflect DNA glycosylase activity because attempted base excision repair of IR damage by the enzyme can lead to lethal and mutagenic DSBs [34].

A variety of untargeted effects may contribute to the short- and long-term fate of a cell exposed to IR [35]. An example is the possible involvement of a "radioadaptive bystander" effect in human lung fibroblasts [36]. The reduction of radiosensitivity in cells with a wild type *p53* gene by a radiation-induced, nitric oxide (NO)-mediated bystander effects may be a manifestation of the radioadaptive response [37,38]. This possibility is supported by the finding that the NO-induced apoptosis observed in lymphoblastoid and fibroblast cells depends on the phosphorylation and activation of p53 [39]. However, it is still unclear whether the NO-mediated pathway also contributes to the mutagenic adaptation. The de novo protein synthesis is required for expression of adaptive responses [22,40], and gene expression studies are improving our understanding of the molecular mechanisms underlying the radioadaptive response [9,10,40,41]. Our laboratory is also focusing on the molecular mechanisms involved in radioadaptation, especially the expression of genes involved in DNA base and nucleotide excision repair.

Acknowledgements

This study was partially supported by the Budget for Nuclear Research of the Ministry of Education, Culture, Sports, Science and Technology, and was reviewed by the Atomic Energy Commission of Japan. We thank Dr. Miriam Bloom (SciWrite Biomedical Writing & Editing Services) for professional editing.

References

[1] G. Olivieri, Y. Bodycote, S. Wolf, Adaptive response of human lymphocytes to low concentrations of radioactive thymidine, Science 223 (1984) 594–597.
[2] S. Wolf, Aspects of the adaptive response to very low doses of radiation and other agents, Mutat. Res. 358 (1996) 135–142.
[3] S. Wolf, The adaptive response in radiobiology: evolving insights and implications, Environ. Health Pesrpect. 106 (1998) 277–283.
[4] O. Rigaud, E. Moustacchi, Radioadaptation for gene mutation and the possible molecular mechanisms of the adaptive response, Mutat. Res. 358 (1996) 127–134.
[5] M. Wojewodska, M. Kruzewski, K. Iwanenko, I. Szumiel, Effects of signal transduction in adapted lymphocytes: micronuclei frequency and DNA repair, Int. J. Radiat. Biol. 71 (1997) 245–252.
[6] P.-K. Zhou, O. Rigaud, Down-regulation of the human *CDC16* gene after exposure to ionizing radiation: a possible role in the radioadaptive response, Radiat. Res. 155 (2001) 43–49.
[7] M.S. Sasaki, Y. Ejima, A. Tachibana, T. Yamada, K. Ishizaki, T. Shimizu, T. Nomura, DNA damage response pathway in radioadaptive response, Mutat. Res. 504 (2002) 101–118.
[8] I. Szumiel, Adaptive responses: stimulated DNA repair or decreased damage fixation? Int. J. Radiat. Biol. 81 (2005) 233–241.
[9] M.A. Coleman, E. Yin, L.E. Peterson, D. Nelson, K. Sorensen, J.D. Tucker, A.J. Wyrobeck, Low-dose irradiation alters the transcript profiles of human lymphoblastoid cells inducing genes associated with radioadaptive response, Radiat. Res. 164 (2005) 369–382.
[10] H.P. Wang, X.H. Long, Z.Z. Sun, O. Rigaud, Q.Z. Xu, Y.C. Huang, J.L. Sui, B. Bai, P.K. Zhou, Identification of differentially transcribed genes in human lymphoblastoid cells irradiated with 0.5 Gy of γ-ray and the involvement of low dose radiation inducible CHD6 gene in cell proliferation and radiosensitivity, Int. J. Radiat. Biol. 82 (2006) 181–190.
[11] S.G. Swant, G. Randers-Pehrson, N.F. Metting, E.J. Hall, Adaptive response and the bystander effect induced by radiation in C3H 10T1/2 cells in culture, Radiat. Res. 156 (2001) 177–180.
[12] H.N. Zhou, G. Randers-Pehrson, C.R. Geard, D.J. Brenner, E.J. Hall, T.K. Hei, Interaction between radiation-induced adaptive response and bystander mutagenesis in mammalian cells, Radiat. Res. 160 (2003) 512–516.
[13] W.M. Bonner, Thresholds, bystander effect, and adaptive response, Proc. Natl. Acad. Sci. U.S.A. 100 (2003) 4973–4975.
[14] S.A. Mitchell, S.A. Marino, D.J. Brenner, E.J. Hall, Bystander effect and adaptive response in C3H 10T(1/2) cells, Int. J. Radiat. Biol. 80 (2004) 465–472.

[15] T.K. Hei, R. Persaud, H. Zhou, M. Suzuki, Genotoxicity in the eyes of bystander cells, Mutat. Res. 568 (2004) 111–120.
[16] T. Ikushima, Chromosomal response to ionizing radiation reminiscent of an adaptive response in cultured Chinese hamster cells, Mutat. Res. 180 (1987) 215–221.
[17] B.J.S. Sanderson, A.A. Morely, Exposure of human lymphocytes to ionizing radiation reduces mutagenicity by subsequent radiation, Mutat. Res. 164 (1986) 151–347.
[18] P.K. Zhou, X.Y. Liu, W.Z. Sun, Y.P. Zhang, Y.P.K. Wei, Cultured mouse SR-1 cells exposed to low-dose of γ-rays become less susceptible to the induction of mutations by radiation as well as bleomycin, Mutagenesis 8 (1993) 109–111.
[19] A.M. Ueno, D.B. Vannais, S.L. Gustafson, J.C. Wong, C.A. Waldren, A low adaptive dose of gamma-rays reduced the number and altered the spectrum of S1 mutants in human hamster hybrid cells, Mutat. Res. 358 (1996) 161–169.
[20] E.I. Azzam, G.P. Raaphorst, R.E. Mitchel, Radiation-induced adaptive response for protection against micronucleus formation and neoplastic transformation in C3H 10T1/2 mouse embryo cells, Radiat. Res. 138 (1994) S28–S31.
[21] O. Rigaud, D. Papadopoulo, E. Moustacchi, Decreased deletion mutation in radioadapted human lymphoblast, Radiat. Res. 133 (1993) 94–101.
[22] T. Ikushima, H. Aritomi, J. Morisita, Radioadaptive response: efficient repair of radiation-induced DNA damage in adapted cells, Mutat. Res. 358 (1996) 193–198.
[23] T.R. Skopek, H.L. Liber, B.W. Penman, W.G. Thilly, Isolation of a human lymphoblastoid line heterozygous at the thymidine kinase locus: possibility for a rapid human cell mutation assay, Biochem. Biophys. Res. Commun. 84 (1978) 411–416.
[24] M. Honma, M. Hayashi, T. Sofuni, Cytotoxic and mutagenic responses to X-rays and chemical mutagens in normal and p53-mutated human lymphoblastoid cell, Mutat. Res. 374 (1996) 89–98.
[25] M. Honma, L.S. Zhang, M. Hayashi, K. Takeshita, Y. Nakagawa, N. Tanaka, T. Sofuni, Illegitimate recombination leading to allelic loss and unbalanced translocation in p53-mutated human lymphoblastoid cells, Mol. Cell. Biol. 17 (1997) 4774–4781.
[26] S. Morimoto, T. Kato, M. Honma, M. Hayashi, F. Hanaoka, F. Yatagai, Detection of genetic alterations induced by low-dose X rays: analysis of loss of heterozygosity for *TK* mutation in human lymphoblastoid cells, Radiat. Res. 157 (2002) 533–538.
[27] S. Morimoto, M. Honma, F. Yatagai, Sensitive detection of LOH events in a human cell line after C-ion beam exposure, J. Radiat. Res. 43 (Suppl.) (2002) S163–S167.
[28] Y. Umebayashi, M. Honma, T. Abe, H. Ryuto, H. Suzuki, T. Shimazu, N. Ishioka, M. Iwaki, F. Yatagai, Mutation induction after low-dose carbon-ion beam irradiation of frozen human cultured cells, Biol. Sci. Space 19 (2005) 237–241.
[29] F. Yatagai, S. Morimoto, T. Kato, M. Honma, Further characterization of loss of heterozygosity enhanced by p53 abrogation in human lymphoblastoid TK6 cells: disappearance of endpoint hotspots, Mutat. Res. 560 (2004) 133–145.
[30] A.J. Grosvsky, B.N. Walter, C.R. Giver, DNA-sequence specificity of mutations at the human thymidine kinase locus, Mutat. Res. 289 (1993) 231–243.
[31] M. Honma, M. Izumi, M. Sakuraba, S. Tadokoro, H. Sakamoto, W. Wang, F. Yatagai, M. Hayashi, Deletion, rearrangement, and gene conversion; genetic consequences of chromosomal double-strand breaks in human cells, Environ. Mol. Mutagen. 42 (2003) 288–298.
[32] Y. Umebayashi, M. Honma, M. Suzuki, H. Suzuki, T. Shimazu, N. Ishioka, M. Iwaki, F. Yatagai, Mutation induction in cultured human cells after low-dose and low-dose-rate γ-ray irradiation: detection by LOH analysis, J. Radiat. Res. 48 (2006) 7–11.
[33] M. Inoue, G.-P. Shen, M.A. Chaudhry, H. Galick, J.O. Blaisdell, S.S. Wallace, Expression of the oxidative base excision repair enzymes is not induced in TK6 human lymphoblastoid cells after low doses of ionizing radiation, Radiat. Res. 161 (2004) 409–417.
[34] N. Yang, H. Galick, S.S. Wallace, Attempted base excision repair of ionizing radiation damage in human lymphoblastoid cells produces lethal and mutagenic double-strand breaks, DNA Repair 3 (2004) 1323–1334.
[35] P.J. Coates, S.A. Lorimore, E.G. Wright, Damaging and protective cell signaling in the untargeted effects of ionizing radiation, Mutat. Res. 568 (2004) 5–20.
[36] R. Iyer, B.E. Lehnert, Low-dose, low-LET ionizing radiation-induced radioadaptation and associated early responses in unirradiated cells, Mutat. Res. 503 (2002) 1–9.
[37] H. Matsumoto, A. Takahashi, T. Ohnishi, Radiation-induced adaptive and bystander effects, Biol. Sci. Space 18 (2004) 247–254.
[38] H. Matsumoto, A. Takahashi, T. Ohnishi, Nitric oxide radicals choreograph a radioadaptive response, Cancer Res. 67 (2007) 8574–8579.
[39] L.M. McLaughlin, B. Demple, Nitric oxide-induced apoptosis in lymphoblastoid and fibroblast cells dependent on the phosphorylation and activation of p53, Cancer Res. 65 (2005) 6097–6104.
[40] J.H. Yongblom, J.K. Wiencke, S. Wolf, Inhibition of the adaptive response of human lymphocytes to very low doses of ionizing radiation by the protein synthesis inhibitor cycloheximide, Mutat. Res. 227 (1989) 257–261.
[41] L.-H. Ding, M. Shingyoji, F. Chen, J.-J. Hwang, S. Burma, C. Lee, J.-F. Chen, D.J. Chen, Gene expression profiles of normal human fibroblasts after exposure to ionizing radiation: a comparative study of low and high doses, Radiat. Res. 164 (2005) 17–26.

BRAIN RESEARCH 1150 (2007) 108–120

available at www.sciencedirect.com

ScienceDirect

www.elsevier.com/locate/brainres

BRAIN RESEARCH

Research Report

β-Estradiol induces synaptogenesis in the hippocampus by enhancing brain-derived neurotrophic factor release from dentate gyrus granule cells

Kaoru Sato[a,*], Tatsuhiro Akaishi[b], Norio Matsuki[c], Yasuo Ohno[a], Ken Nakazawa[a]

[a]Division of Pharmacology, National Institute of Health Sciences, 1-18-1 Kamiyoga, Setagaya-ku, Tokyo 158-8501, Japan
[b]Laboratory of Pharmacology, Faculty of Pharmacy and Research Institute of Pharmaceutical Sciences, Musashino University, 1-1-20 Shinmachi, Nishitokyo-shi, Tokyo 202-8585, Japan
[c]Laboratory of Chemical Pharmacology, Graduate School of Pharmaceutical Sciences, University of Tokyo, 7-3-1 Hongo, Bunkyo-ku, Tokyo 113-0033, Japan

ARTICLE INFO

Article history:
Accepted 28 February 2007
Available online 13 March 2007

Keywords:
β-Estradiol
Organotypic hippocampal slice culture
Dentate gyrus
CA3
Synaptogenesis
BDNF

ABSTRACT

We investigated the effect of β-estradiol (E2) on synaptogenesis in the hippocampus using organotypic hippocampal slice cultures and subregional hippocampal neuron cultures. E2 increased the expression of PSD95, a postsynaptic marker, specifically in stratum lucidum of Cornu Ammonis 3 (CA3SL) in cultured hippocampal slices. E2 also increased the spine density at the proximal site of CA3 apical dendrites in CA3SL and PSD95 was clustered on these spine heads. The effects of E2 on the expression of PSD95 and the spine density disappeared when the dentate gyrus (DG) had been excised at 1 day in vitro (DIV). FM1-43 analysis of subregional hippocampal neuron cultures which were comprised of Ammon's horn neurons, DG neurons, or a mixture of these neurons, revealed that E2 increased the number of presynaptic sites in the cultures that contained DG neurons. K252a, a potent inhibitor of the high affinity receptor of brain-derived neurotrophic factor (BDNF), and function-blocking antibody to BDNF (BDNFAB) completely inhibited the effects of E2 in hippocampal slice cultures and subregional neuron cultures, whereas ICI182,780 (ICI), a strong antagonist of nuclear estrogen receptors (nERs), did not. Expression of BDNF in DG neurons was markedly higher than that in Ammon's horn

* *Corresponding author.* Fax: +81 3 3707 6950.
E-mail address: kasato@nihs.go.jp (K. Sato).

Abbreviations: ACM, astrocyte-conditioned medium; ANOVA, analysis of variance; AraC, cytosine β-D-arabino-furanoside; BDNF, brain-derived neurotrophic factor; BDNFAB, function blocking antibody to BDNF; BSA, bovine serum albumin; CA1, Cornu Ammonis 1; CA3, Cornu Ammonis 3; cAMP, 3′–5′-cyclic adenosine monophosphate; CNS, central nervous system; CREB, PKA/cAMP-responsive element binding protein; DG, dentate gyrus; DIC, differential interference contrast; DiI, 1,1′-dioctadecyl-3,3,3′,3′-tetramethylindocarbocyanine perchlorate; DIV, day(s) in vitro; DMSO, dimethylsufoxide; E2, β-estradiol; ECL, enhanced chemiluminescence; EDTA, ethylenediaminetetraacetic acid; ELISA, enzyme linked immunosorbent assay; ER, estrogen receptor; FM1-43, (*N*-(3-triethylammoniumpropyl)-4-(4-(dibutylamino)styryl)pyridinium dibromide; GABA, γ(gamma)-aminobutyric acid; HBSS, Hank's balanced salt solution; HS, horse serum; ICI, ICI182,780; IgG, immunoglobulin G; LDCVs, large dense-core vesicles; L-Glu, L-glutamate; LTP, long-term-potentiation; MEK, MAP kinase kinase; MEM, minimal essential medium; mER, membrane estrogen receptor; NB, neurobasal medium; nER, nuclear estrogen receptor; NeuN, neuronal nuclear antigen; OD, optical density; P3, postnatal day 3; P8, postnatal day 8; PB, phosphate buffer; PBS, phosphate buffered saline; PDZ, PSD-95-Disks large-zona occludens 1/2; PFA, paraformaldehyde; PKA, cAMP-dependent protein kinase A; PSD95, postsynaptic density protein of 95 kDa; Rp-cAMP, Rp-adenosine 3′, 5′-cyclic monophosphorothioate triethylammonium salt; SDS, sodium dodecyl sulphate; S.E.M., standard error of the mean; SL, stratum lucidum; SO, stratum oliens; SP, stratum pyramidale; SR, stratum radiatum; TBS, Tris-buffered saline; TrkB, the high affinity receptor for several neurotrophins; TTX, tetrodotoxin

0006-8993/$ – see front matter
doi:10.1016/j.brainres.2007.02.093

neurons and E2 did not affect these expression levels. E2 significantly increased the BDNF release from DG neurons. KT5720, a specific inhibitor of 3′–5′-cyclic adenosine monophosphate (cAMP)-dependent protein kinase A (PKA), and Rp-adenosine 3′, 5′-cyclic monophosphorothioate triethylammonium salt (Rp-cAMP), a non-hydrolyzable diastereoisomer and a potent inhibitor of PKA, completely suppressed the E2-induced increase in BDNF release, whereas ICI and U0126, a potent inhibitor of MAP kinase kinase (MEK), did not. These results suggest that E2 induces synaptogenesis between mossy fibers and CA3 neurons by enhancing BDNF release from DG granule cells in a nER-independent and PKA-dependent manner.

1. Introduction

Estrogens have diverse effects on structure and function of the central nervous system (CNS) (for review, McEwen et al., 2001; Scharfman and MacLusky, 2005; Segal and Murphy, 2001). These effects include enhancement of glutamate-mediated transmission (Woolley, 1998), decreased afterhyperpolarization (Kramar et al., 2004), facilitation of memory (Tyler et al., 2002), increased dendritic spine and spine synapse numbers (Segal and Murphy, 2001), promotion of DG neurogenesis (Tanapat et al., 1999), and increased seizure susceptibility (Woolley and Schwartzkroin, 1998). Such diversity arises because estrogens have multiple mechanisms of action. They modulate gene transcription by interacting with 2 types of nERs, ERα and ERβ. In addition, recent reports clarified nongenomic mechanisms that act via receptors associated

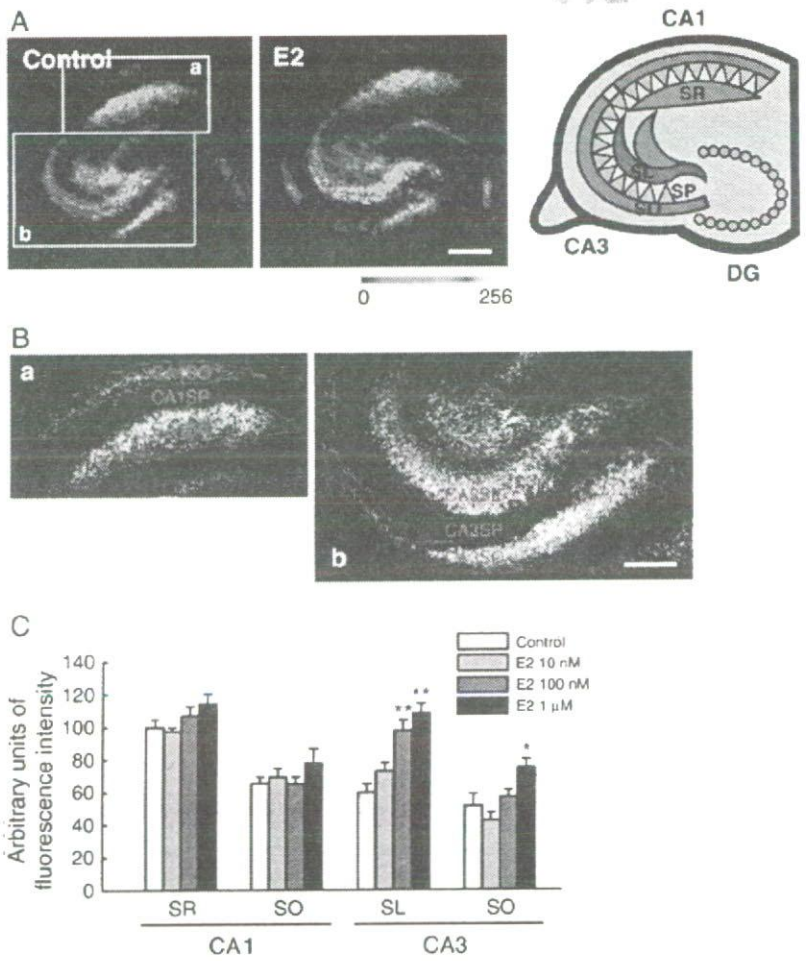

Fig. 1 – Effects of E2 on the expression of PSD95 in cultured hippocampal slices. (A) PSD95 immunoreactive signals in the control slice (left) and the slice treated with E2 (1 μM, 24 h) (middle). Bar=500 μm. (B) Magnified gray-scale images of a and b in A. CA1SR, CA1SO, CA3SL, and CA3SO appeared as fluorescent compartments. Bar=250 μm. (C) Effects of E2 (10 nM–1 μM, 24 h) on the expression of PSD95. E2 increased the expression level of PSD95 dose-dependently in CA3SL. *: $p<0.05$, **: $p<0.01$ vs. the control group in each region. $N=8$, Tukey's test following ANOVA.

with or integral to plasma membrane (mERs), thereby activating signaling cascades distinct from those of nERs (Beyer et al., 2003; Kelly and Levin, 2001; Segars and Driggers, 2002). We previously reported that pretreatment with estrogens increased neuronal sensitivity to L-glutamate (L-glu) specifically in CA3 in organotypic hippocampal slice cultures. In the same study we found that these effects were mediated by the mechanisms that did not involve nERs (Sato et al., 2002). These results raised the possibility that estrogens affect synaptic contacts in CA3. In the present study, we therefore investigated the effects of E2 on synaptogenesis in the hippocampus and explored the underlying mechanisms using 2 experimental systems. Firstly, we investigated the effects of E2 on the expression of PSD95, a postsynaptic marker, and the spine density in cultured hippocampal slices. Secondly, we investigated the effects of E2 on the number of presynaptic release sites in subregional hippocampal neuron cultures, which were comprised of Ammon's horn neurons, DG neurons, or a mixture of these neurons. It has been reported that in the hippocampus the highest concentration of BDNF occurs in DG granule cells, especially in their axons, mossy fibers (Dieni and Rees, 2002; Scharfman et al., 2003), from the prenatal period through to adulthood (Dieni and Rees, 2002). Although BDNF is known to promote synaptogenesis (Aguado et al., 2003; Alsina et al., 2001; Seil and Drake-Baumann, 2000), it has not been elucidated whether the BDNF in DG granule cells has a role in hippocampal synapse formation. For this reason, we also investigated the relationship between endogenous BDNF in DG granule cells and the effects of E2 in CA3. We here provide evidence showing that E2 induces synaptogenesis between mossy fibers and CA3 neurons by enhancing BDNF release from DG granule cells in a nER-independent and PKA-dependent manner.

2. Results

2.1. *Effects of E2 on postsynaptic sites in cultured hippocampal slices*

We first examined the effect of E2 on the expression of PSD95 in cultured hippocampal slices immunohistochemically. PSD95 is one of the PDZ (PSD-95-Disks large-zona occludens 1/2) domain-containing proteins (Craven and Bredt, 1998; Garner et al., 2000) and is an integral protein of the postsynaptic density. In the control group, the fluorescent signals for PSD95 were apparent in the major hippocampal synaptic sites, i.e., stratum radiatum (SR), stratum oriens (SO), SL and the dentate hilar region (Fig. 1A, left). Because in this study slices were cultured after removing entorhinal cortex, we quantified the expression of PSD95 in CA1SR, CA1SO, CA3SL, and CA3SO, the synaptic sites which maintain the intact presynaptic and postsynaptic cells. Because CA1SR, CA1SO, CA3SL, and CA3SO appeared as fluorescent compartments (Figs. 1B, a and b) in magnified gray-scale mode images, we regarded the averaged fluorescence intensity of each compartment (an outlined area) as the expression level of PSD95 of each synaptic site (see Experimental procedures). When we compared the effects of E2 on the PSD95 expression in CA1 and CA3, E2 (24 h) increased the expression of PSD95 dose-dependently in CA3SL and the effects were significant at 100 nM and the higher concentration (Figs. 1A middle and B). Although E2 also increased the PSD 95 expression in CA3SO at 1 μM (145±9.75% of control), the effect was weaker than that in CA3SL (180±10.2% of control at 1 μM). The distribution pattern of PSD95 signals (including area) in each region was not affected by E2. We then investigated the effect of E2 on the spine density in CA3SL using 1,1′-dioctadecyl-3,3,3′,3′-tetramethylindocarbocyanine perchlorate (DiI) staining. E2 (1 μM, 24 h) markedly increased the spine density at the proximal site of CA3 apical dendrites in CA3SL (296±24.3% of control; Figs. 2A and B). E2 also increased the spine density at the proximal site of CA1 apical dendrites in CA1SR (132±4.49% of control), although to a much lesser extent than that in CA3SL (Fig. 2A). Fig. 2B shows typical images of the proximal sites of CA3 apical dendrites in the control slice (left) and in the E2-treated slice (right). When we immunostained the E2-treated slices with anti-PSD95 antibody after DiI staining, most PSD95 signals in CA3SL clustered on the spine heads (Fig. 2B, right). These results indicate that E2 increased the number of postsynaptic sites in CA3SL. CA3SL is the region in which mossy fibers (DG granule cell axons) make synapses with CA3 pyramidal neurons. We then investigated the effect of E2 on the expression of PSD95 and the spine density in CA3 in DG (−) slices, i.e., the slices of which DG had been excised at 1 DIV. As shown by

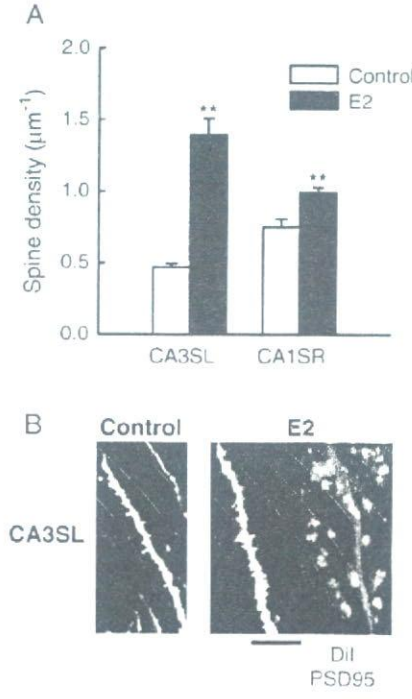

Fig. 2 – Effects of E2 on the spine density in cultured hippocampal slices. (A) E2 (1 μM, 24 h) markedly increased the spine density in CA3SL. **: $p<0.01$ vs. the vehicle control group in each region. $N=8$, Student's t test. (B) Typical images of the DiI-labeled CA3 apical dendrites in the control slice (left) and the E2-treated slice (right). Double staining with DiI and anti-PSD95 antibody revealed that in the E2-treated slice most PSD95 signals (green) were clustered on the spine-heads of the CA3 apical dendrites (red). Bar=5 μm.

Nissl staining, the viability of CA3 pyramidal neurons was not altered by the dissection of the DG (Fig. 3A). The distribution pattern of the PSD95 signals was not affected, either (Fig. 3B). E2 (1 μM, 24 h) affected neither the expression level (Fig. 3C) nor the distribution pattern of PSD95 in DG (–) slices (data not shown). The effect of E2 (1 μM, 24 h) on the spine density in CA3SL was also abolished in DG (–) slices (Fig. 3D). Taken together, these results suggest that E2 induces synaptogenesis between mossy fibers and CA3 pyramidal neurons.

2.2. *Effects of E2 on presynaptic sites in subregional hippocampal neuron cultures*

We next investigated the effect of E2 on the number of presynaptic sites using subregional hippocampal neuron cultures, which were comprised of Ammon's horn neurons, DG neurons, or a mixture of these neurons, respectively. We quantified the number of presynaptic sites by counting the number of sites in which depolarization-induced uptake and release of (*N*-(3-triethylammoniumpropyl)-4-(4-(dibutylamino)styryl)pyridinium dibromide (FM1-43) (Cochilla et al., 1999) had occurred (see Experimental procedures). Fig. 4A shows the typical morphologies of neurons in the Ammon's horn neuron culture (left) and in the DG neuron culture (middle). Most cells in the Ammon's horn neuron culture were large and spindle-shaped, whereas most cells in the DG neuron culture were small and granular. As shown in Fig. 4B, E2 (1 μM, 24 h) significantly increased the number of presynaptic sites in the mixed neuron culture (199±9.18% of control). E2 also increased the number of presynaptic sites in the DG neuron culture (170±12.1% of control), but not in the Ammon's horn neuron culture. Fig. 4C shows the typical fluorescent images of presynaptic sites (red puncta) in the control group (top left) and in the E2-treated group (top right) in the mixed neuron culture. We confirmed that E2 had no effect on the number of surviving neurons in each culture by immunostaining with anti-NeuN antibody (data not shown). These results indicate that E2 increased the number of presynaptic sites in the hippocampal neuron cultures and that DG neurons are indispensable for this effect.

2.3. *The effects of E2 in hippocampal slice cultures and subregional hippocampal neuron cultures were mediated by the mechanism which is independent of nERs and dependent on endogenous BDNF*

Pharmacological experiments were performed to investigate and compare the mechanisms underlying the effects of E2 in hippocampal slice cultures and subregional hippocampal neuron cultures (the mixed neuron culture) (Fig. 5). First, we examined the contribution of nERs using ICI, a strong antagonist to both of ERα (Ki: 1.5 nM) and ERβ (Ki: 6.4 nM) (Kuiper et al., 1997). ICI at a concentration of 1 μM did not alter the effect of E2 on the expression of PSD95 expression, the spine density, and the number of presynaptic sites (Figs. 5A–C). It has been reported that DG granule cells have the highest concentration of BDNF in the hippocampus, especially in the mossy fibers (Dieni and Rees, 2002; Scharfman et al., 2003). Because BDNF is known to enhance synapse formation (Aguado et al., 2003; Alsina et al., 2001; Seil and Drake-

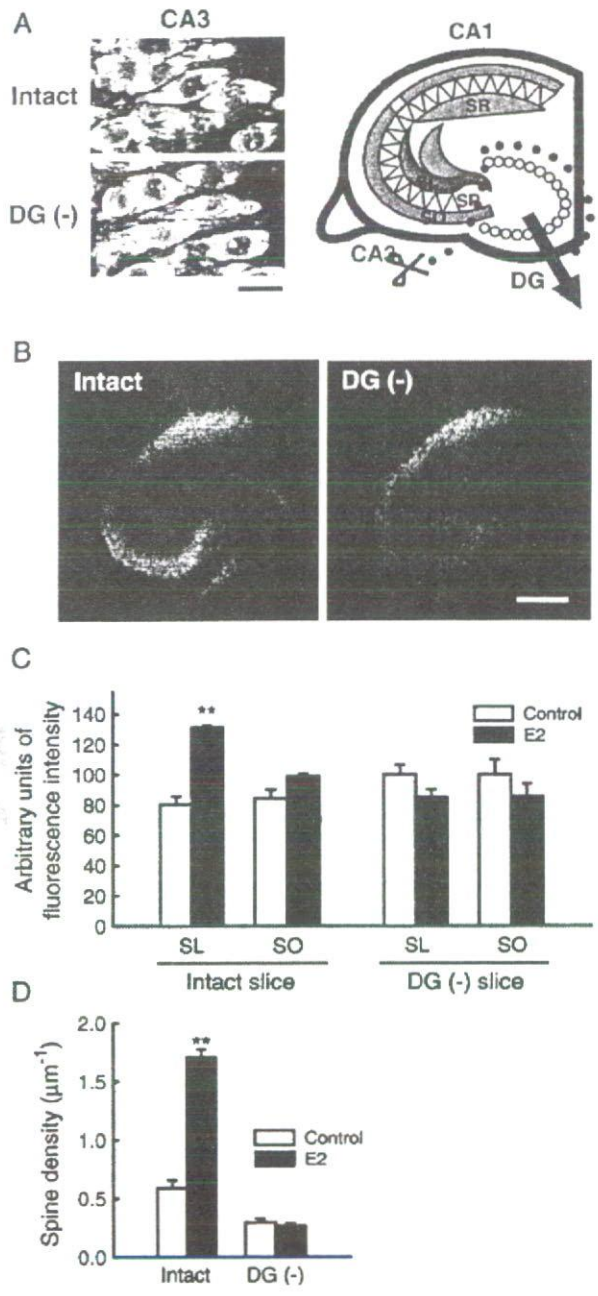

Fig. 3 – Effects of E2 on the expression of PSD95 and the spine density in cultured hippocampal slices of which DG had been excised at 1 DIV. (A) The viability of CA3 pyramidal neurons in DG (–) slices. Nissl staining revealed that their viability was not affected by the dissection of DG. Bar=20 μm. (B) Immunoreactive signals of PSD95 in a DG (–) slice. The distribution pattern of the PSD95 signals was not affected by the dissection of DG. Bar=500 μm. (C) The effect of E2 on the expression of PSD95 in DG (–) slices. E2 (1 μM, 24 h) did not affect the expression of PSD95 in CA3 in DG (–) slices. (D) The effect of E2 on the spine density in CA3SL in DG (–) slices. E2 (1 μM, 24 h) did not affect the spine density in CA3SL in DG (–) slices.

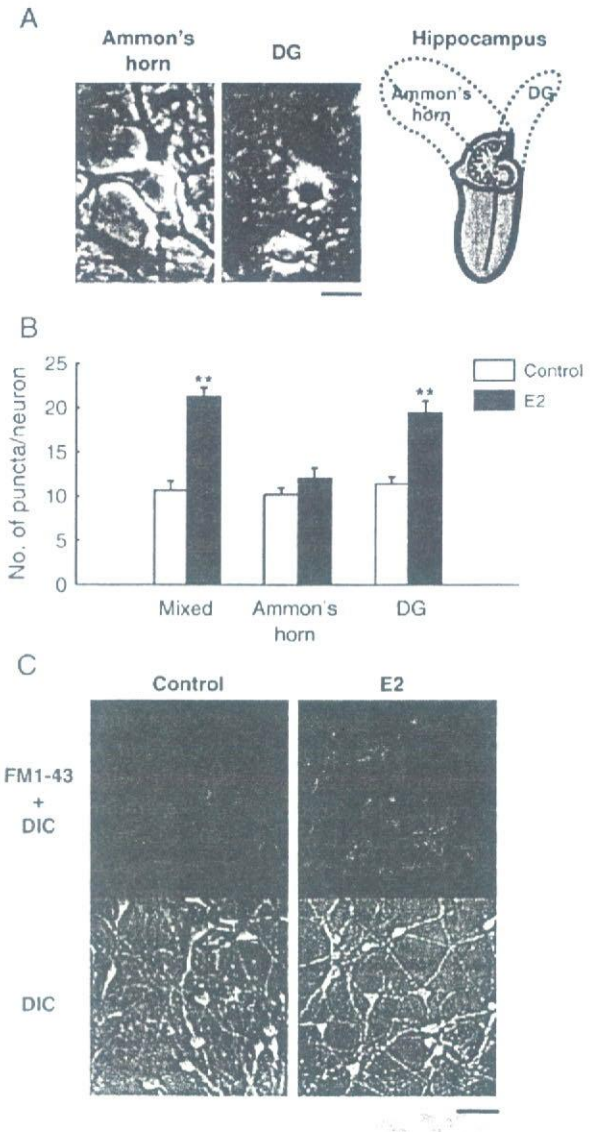

Fig. 4 – Effects of E2 on the number of presynaptic sites in subregional hippocampal neuron cultures. (A) Typical cell morphologies in the Ammon's horn neuron culture (left) and in the DG neuron culture (middle). Bar=20 μm. (B) E2 (1 μM, 24 h) significantly increased the number of presynaptic sites in the mixed neuron culture and in the DG neuron culture. **: $p<0.01$ vs. the control group in each culture. $N=8$, Student's t test. (C) Typical images of presynaptic sites visualized by FM1-43 (red puncta) in the control group (top left) and in the E2-treated group (top right) in the mixed neuron culture. DIC images of the same microscopic views were also shown (bottom left and bottom right). Bar=50 μm.

Baumann, 2000), we examined the involvement of BDNF in the effects of E2. K252a (200 nM), a potent inhibitor of the high affinity receptor of BDNF (TrkB) (Squinto et al., 1991; Bothwell, 1995), significantly inhibited the effects of E2 on the expression of PSD95 expression, the spine density, and the number of presynaptic sites (Figs. 5A–C). Furthermore BDNFAB (10 μg/ml) significantly inhibited the effects of E2 in these experiments (Figs. 5A–C). These inhibitors alone had no effects in each case. These results indicate that the effects of E2 in hippocampal

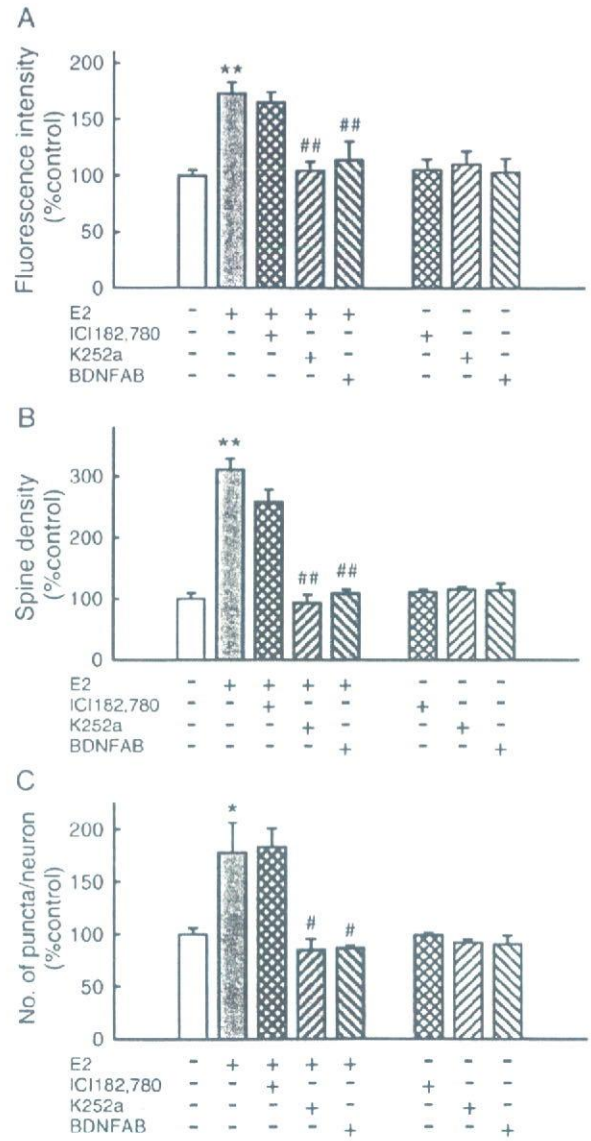

Fig. 5 – Effects of ICI, K252a, and BDNFAB on the effects of E2 in hippocampal slice cultures and subregional hippocampal neuron cultures. (A) K252a (200 nM) and BDNFAB (10 μg/ml) significantly inhibited the effect of E2 on the expression of PSD95 in cultured hippocampal slices, whereas ICI (1 μM) did not. **: $p<0.01$ vs. the control group, ##: $p<0.01$ vs. the E2-treated group. $N=8$, Tukey's test following ANOVA. (B) K252a (200 nM) and BDNFAB (10 μg/ml) significantly inhibited the effect of E2 on the spine density in cultured hippocampal slices, whereas ICI (1 μM) did not. **: $p<0.01$ vs. the control group, ##: $p<0.01$ vs. the E2-treated group. $N=8$, Tukey's test following ANOVA. (C) K252a (200 nM) and BDNFAB (10 μg/ml) significantly inhibited the effect of E2 on the number of presynaptic sites in the mixed neuron culture, whereas ICI (1 μM) did not. *: $p<0.05$ vs. the control group, #: $p<0.05$ vs. the E2-treated group. $N=8$, Tukey's test following ANOVA.

slice cultures and subregional neuron cultures were mediated by the common mechanism which is independent of nERs and dependent on endogenous BDNF, suggesting the involvement of BDNF in DG granule cells in the synaptogenic effect of E2 in CA3SL.

2.4. *E2 enhanced BDNF release from DG granule cells via nER-independent and PKA-dependent mechanisms*

We further examined the association between the effects of E2 and BDNF using subregional hippocampal neuron cultures. The expression levels of BDNF were confirmed for both the Ammon's horn neuron culture and the DG neuron culture by Western blot analysis and enzyme linked immunosorbent assay (ELISA) (Fig. 6). In Western blot analysis, BDNF immunoreactive bands were detected in the control lanes for both cultures, but the OD for the DG neurons was markedly higher than that for the Ammon's horn neurons (Fig. 6A). E2 (1 μM, 24 h) did not affect the expression levels of BNDF in Ammon's horn neurons or DG neurons. ELISA also showed that the expression level of BDNF in DG neurons was remarkably higher than that of Ammon's horn neurons and E2 had no effect on the expression levels in both cultures (Fig. 6B). These results indicate that subregional neuron cultures reflect in vivo pattern of BDNF expression in the hippocampus, in which the highest concentration of BDNF occurs in DG granule cells (Dieni and Rees, 2002; Scharfman et al., 2003). We next examined the possibility that E2 enhances BDNF release from DG granule cells without affecting BDNF expression. The amount of BDNF released into the culture medium of the DG neuron culture was measured by ELISA. We performed ELISA after 10 h of treatment with E2, at the time point when the effect of E2 on the number of presynaptic sites was not yet apparent (Fig. 7A). E2 (1 μM, 10 h) remarkably increased the BDNF release (267 ± 20.5% of control; Fig. 7B). Neither ICI (1 μM) nor U0126 (10 μM) (Ki: 72 nM for MEK1, 58 nM for MEK2) (Duncia et al., 1998), influenced the effect of E2. In contrast, KT5720 (200 nM) (Ki: 56 nM for PKA) (Kase et al., 1987) and Rp-cAMP (10 μM) (Ki: 11 μM for PKA) (Rothermel and Parker Botelho, 1988), suppressed the effect of E2 to the control level. These inhibitors alone had no effects on the basal BDNF release. These results indicate that E2 enhanced BDNF release from DG

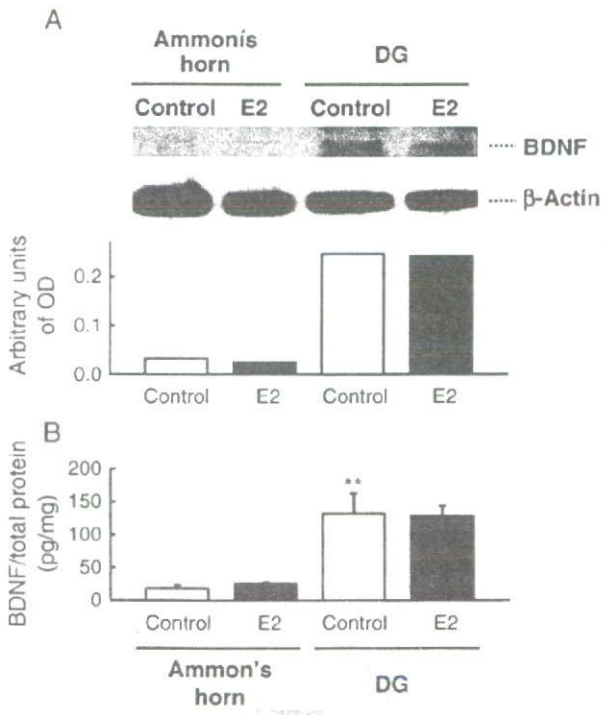

Fig. 6 – The expression of BDNF in subregional hippocampal neuron cultures. (A) Western blot analysis of BDNF in subregional hippocampal neuron cultures. The expression level of BDNF of DG neurons was much higher than that of Ammon's horn neurons. E2 (1 μM, 24 h) had no effect on the BDNF expression level. The same results were obtained in 3 independent experiments. (B) ELISA detection of BDNF in subregional hippocampal neuron cultures. The expression level of BDNF in DG neurons was significantly higher than that in Ammon's horn neurons. E2 (1 μM, 24 h) had no effect on the BDNF expression level. **: $p<0.01$ vs. the control group of Ammon's horn neurons. $N=4$, Tukey's test following ANOVA.

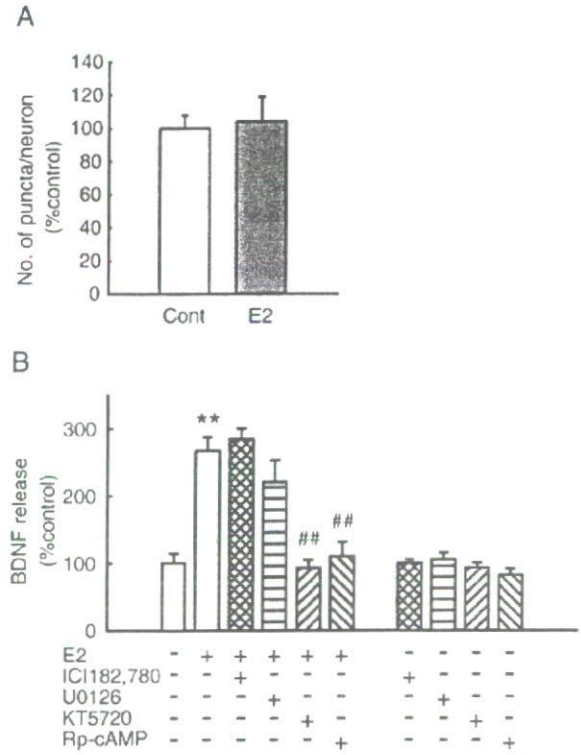

Fig. 7 – Effects of E2 on the BDNF release in the DG neuron culture. (A) Treatment for 10 h with E2 (1 μM) had no effect on the number of presynaptic sites in the DG neuron culture. (B) E2 (1 μM, 10 h) significantly enhanced BDNF release in the DG neuron culture. KT5720 (200 nM) and Rp-cAMP (10 μM) inhibited the effect of E2, whereas ICI (1 μM) and U0126 (10 μM) did not. **: $p<0.01$ vs. the control group, ##: $p<0.01$ vs. the E2-treated group. $N=4$, Tukey's test following ANOVA.

granule cells via nER-independent and PKA-dependent mechanisms, which may underlie the effects of E2 described above.

3. Discussion

In this study, we provided evidence showing that E2 induces synaptogenesis between mossy fibers and CA3 neurons by enhancing BDNF release from DG granule cells in a nER-independent and PKA-dependent manner.

We used subregional hippocampal neuron cultures to investigate the effects of E2 in detail. That these cultures sufficiently maintain their region-specific characters is supported by the following evidence: 1) the morphology of neurons in the Ammon's horn neuron culture was clearly different from that in the DG neuron culture (Fig. 4A). Most cells in the Ammon's horn neuron culture were large and spindle-shaped, which is typical for pyramidal neurons. Most cells in the DG neuron culture were small and granular, which is typical for DG granule cells. 2) DG neurons isolated and cultured using a similar procedure maintain their in vivo physiological properties (Ikegaya et al., 2000). 3) The expression level of BDNF of the cultured DG neurons is much higher than that of the cultured Ammon's horn neurons, reflecting in vivo pattern of BDNF expression in the hippocampus, in which the highest concentration of BDNF occurs in DG granule cells (Dieni and Rees, 2002; Scharfman et al., 2003).

In our study, we prepared hippocampal slices from both genders of P8 rat pups and cultured for 10 days with medium supplemented with horse serum (HS) collected from gelding horses, in which steroid concentrations were under the limits for detection. Because the increases in the expression level of PSD95 and the spine density in CA3 were observed in all slices treated with E2, we consider that the effects of E2 in our study are gender-independent. Currently we are investigating whether or not there is gender difference in the extents of the effects of E2. Organotypic hippocampal slice cultures of P5–9 rat brains are well-established, stable model for investigating hippocampal function including developmental synaptogenesis because neurons maintain synaptogenic ability in each region (CA1, CA3, and DG) (De Simoni et al., 2003; Mizuhashi et al., 2001; Qin et al., 2001). It has been reported that during postnatal development, the capacity of estrogen binding protein is high enough to lower the concentrations of serum estrogens to nonphysiological levels (Germain et al., 1978). This suggests that the conditions for the hippocampal slice culture in the present study more closely represent the postnatal developmental stage. Recently it was clarified that E2 is synthesized from endogenous cholesterol by P45017α and P450 aromatase in hippocampal neurons (Hojo et al., 2004) and that it plays an essential role in the maintenance of synapses (Kretz et al., 2004). The effects of E2 shown here might be achieved by locally synthesized E2 at the postnatal developmental stage. Two previous studies reported the effects of E2 on spinogenesis in cultured hippocampal slices (Kretz et al., 2004; Pozzo-Miller et al., 1999), but their results are conflicting, perhaps because of the effects of various steroids included in the HS in the culture medium.

Our findings suggest that BDNF in DG granule cells mediates the effects of E2. It has been reported that in the hippocampus the highest concentration of BDNF occurs in DG granule cells, especially in their axons, mossy fibers (Dieni and Rees, 2002; Scharfman et al., 2003), from the prenatal period through to adulthood (Dieni and Rees, 2002). The significance of BDNF in DG granule cells, however, had been unknown until Scharfman et al. showed that endogenous BDNF in mossy fibers affected the excitability of CA3 neurons in adult female rats (Scharfman et al., 2003). On the other hand, BDNF has long been known to promote synaptogenesis by maturation of presynaptic sites (Aguado et al., 2003; Seil and Drake-Baumann, 2000). Real-time monitoring revealed that BDNF increases the number of presynaptic sites (Alsina et al., 2001). Presynaptic maturation can induce postsynaptic maturation, as shown by mossy fiber induction of postsynaptic maturation including assembly and clustering of PSD95 on CA3 apical dendrites (Qin et al., 2001). In the present study, BDNF released from DG granule cells may have first increased the number of presynaptic sites by autocrine/paracrine mechanisms, thereby inducing the maturation of postsynaptic sites. In addition to the communication with CA3 pyramidal neurons through giant boutons, mossy fibers also communicate with local circuit interneurons in CA3 through filopodial extensions and en passant boutons (Acsady et al., 1998; Lawrence and McBain, 2003). Although the number of these small terminals is greater than that of giant boutons, we consider that E2 predominantly promoted the synaptogenesis between mossy fibers and CA3 pyramidal neurons in this study because of the following reasons: 1) E2 increased the number of giant boutons, which were identified as mossy fiber terminals containing Zn^{2+} in our previous report (Sato et al., 2002), and 2) the major population of BDNF-positive mossy fiber terminals is those with giant boutons (Danzer and McNamara, 2004). Further experiments using interneuron-specific markers will be necessary to identify the effect of E2 on synaptogenesis between mossy fibers and CA3 interneurons.

E2 enhanced BDNF release from DG granule cells in a nER-independent and PKA-dependent manner. Besides the genomic effects via nERs (ERα and ERβ), recent reports have described the nongenomic effects of estrogens mediated by mERs (Beyer et al., 2003; Kelly and Levin, 2001; Segars and Driggers, 2002). Although the membrane localization of the E2 binding sites is widely accepted, mERs still await isolation and gene cloning. One of the candidate mERs is membrane-localized ERα/β that can activate signal transduction pathways distinct from nERα/β (Razandi et al., 2004; Thomas et al., 2004). Although the mode of action has not been elucidated precisely, ERα has been localized to the neuronal plasma membrane in the hippocampus (Clarke et al., 2000). On the other hand, several reports suggest that the proteins, which are completely different from ERα/β, function as mERs in hypothalamus (Cambiasso and Carrer, 2001), midbrain (Beyer and Karolczak, 2000; Beyer et al., 2002), and neocortex (Toran-Allerand et al., 2002). The effects of E2 observed in our study may have been mediated by one or more mechanisms other than nERs.

It has been reported that E2 modulates the expression of BDNF by genomic (Sohrabji et al., 1995) or nongenomic mechanisms (Ivanova et al., 2001). Unexpectedly, in this